JIRRS
Journal International Review of Research Studies

Received: 02/05/2026 - **Accepted:** 07/07/2026
Vol: 01.09
DOI: 10.66104/dempc459
Pages: 1-30

BALANCING NICKEL RECOVERY, IRON DISSOLUTION, ACID DOSAGE, AND RESIDENCE TIME IN ATMOSPHERIC SULFURIC ACID LEACHING OF A FERRUGINOUS LATERITIC NICKEL ORE

Antonio Clareti Pereira, PhD
PhD in Chemical Engineering
University of São Paulo (USP)
Belo Horizonte, Minas Gerais, Brazil
E-mail: claretipereira@gmail.com
ORCID: https://orcid.org/0000-0001-8115-4279

Abstract

Atmospheric sulfuric acid leaching of ferruginous lateritic nickel ores requires a compromise between nickel recovery, iron dissolution, acid dosage, and residence time. In this study, a limonitic nickel ore fraction retained at 100 mesh was leached at approximately 95-100 °C using 700-1000 kg H_2SO_4/t ore while maintaining a constant initial slurry mass and solid-liquid basis. The ore contained approximately 1.08 wt.% Ni and 33.53 wt.% Fe, and mineralogical characterization indicated that nickel was mainly associated with iron oxyhydroxides, Si-Fe plasma, and subordinate phyllosilicates. Corrected extraction values showed that nickel extraction increased with acid dosage and residence time, reaching 84.9% at 700 kg/t and 420 min, 89.3% at 800 kg/t and 420 min, and 91.0% at 900 kg/t and 420 min. However, iron dissolution also increased, particularly at higher acid dosages. The 1000 kg/t condition was retained from 240 to 420 min after recalculation by direct liquid-wash-residue mass balance; it reached 83.1-89.5% Ni but dissolved 71.3-80.4% Fe, indicating severe loss of selectivity. Apparent pseudo-first-order and shrinking-core-type models were used as diagnostic tools, not as definitive mechanistic proof. A process-oriented acid-Fe-time penalty index was developed to rank feasible operating conditions. The preferred screening condition was 800 kg H_2SO_4/t ore and 300 min, achieving 82.8% Ni extraction with 48.4% Fe dissolution while avoiding higher acid and residence-time penalties. The framework is intended for screening and ranking operating windows, not for final plant design or economic optimization.

Keywords: nickel laterite; atmospheric leaching; sulfuric acid; iron dissolution; acid dosage; residence time; leaching kinetics; shrinking-core model; process decision index; hydrometallurgical screening.

Highlights

- Corrected extraction values were incorporated for the 700-900 kg H_2SO_4/t ore tests.
- The 1000 kg H_2SO_4/t ore test was retained from 240 to 420 min using recalculated mass-balance values.
- The 1000 kg/t condition achieved high Ni extraction but dissolved excessive Fe.
- Kinetic models were used as comparative diagnostic tools, not as proof of a unique mechanism.
- An acid-Fe-time penalty index supports identifying 800 kg H_2SO_4/t ore and 300 min as the preferred screening condition.

Graphical abstract

JIRRS
Journal International Review of Research Studies

Received: 02/05/2026 - **Accepted:** 07/07/2026
Vol: 01.09
DOI: 10.66104/dempc459
Pages: 1-30

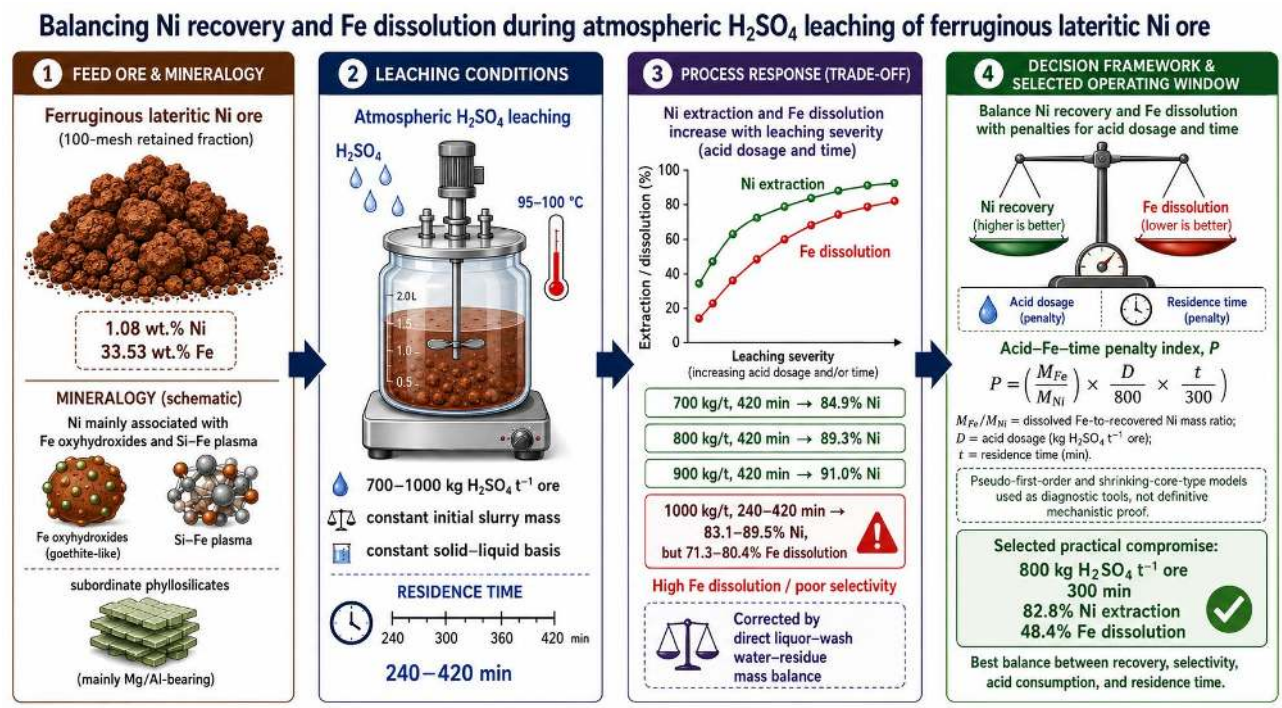

1. Introduction

Lateritic nickel ores are increasingly important for the supply of nickel and cobalt, but their processing route depends strongly on the limonite/saprolite balance, the abundance of iron-rich phases, and the acid-consuming gangue. Reviews of laterite processing show that atmospheric leaching, high-pressure acid leaching, heap/vat leaching, sulfation-roasting-leaching, and hybrid hydrometallurgical schemes are best understood as ore-specific flowsheet options rather than interchangeable technologies (Stanković et al., 2020; Bahfie et al., 2022; Pandey et al., 2023; Chi et al., 2026; Acquah et al., 2026).

Atmospheric sulfuric acid leaching has been widely evaluated for limonitic and iron-rich laterites because it avoids autoclave pressure, but it must contend with the inherent trade-off between Ni/Co recovery and the dissolution of Fe, Mg, Al, Mn, Cr, and other impurities. Prior studies on atmospheric sulfuric acid leaching and related kinetic evaluation provide the direct background for the present work (Hosseini Nasab et al., 2020; Santos et al., 2021; Safitri et al., 2021; Astuti et al., 2024; Prasetya et al., 2025; Ribeiro et al., 2025; Ma et al., 2026). Comparative work on limonitic and saprolitic ores also shows that the same nominal leaching condition may behave differently depending on mineralogy, particle size, temperature, and ore texture (Jeong et al., 2025; Kang et al., 2026).

Iron is a central process constraint in the leaching of limonitic laterite. Dissolved Fe consumes acid directly and indirectly, increases neutralization demand, promotes generation of Fe-

JIRRS
Journal International Review of Research Studies
Received: 02/05/2026 - **Accepted:** 07/07/2026
Vol: 01.09
DOI: 10.66104/dempc459
Pages: 1-30

rich precipitates, and can complicate solid-liquid separation. The importance of Fe control is evident both in leaching studies and in subsequent Fe precipitation strategies from nickel laterite leach liquors (da Silva et al., 2022; Setiawan et al., 2024; Ma et al., 2026). Therefore, process selection should not be based only on maximum Ni extraction; it should also penalize excessive Fe dissolution and reagent intensity.

Several approaches have been proposed to improve extraction or selectivity, including pre-roasting, sulfation roasting, water leaching, ammonia leaching, solvent extraction, mechanical activation, microwave-assisted leaching, combined organic and inorganic acid systems, and integrated SO_3 recovery concepts (Dahani et al., 2020; Ribeiro et al., 2020; Ribeiro et al., 2021; Yunita & Mubarok, 2021; Hariyanto et al., 2023; Li et al., 2023; Acquah et al., 2025; Prameswara et al., 2024; Li et al., 2026; Osali et al., 2026; Tyassena et al., 2026; Zhao et al., 2024). These studies demonstrate that higher extraction can often be achieved, but the process penalty may shift to acid consumption, roasting energy, reagent complexity, downstream purification, or equipment cost.

Mineralogical characterization is essential because nickel may be hosted in goethite/iron oxyhydroxides, siliceous-ferruginous plasma, phyllosilicates, serpentine-related phases, and Mn oxides, depending on the lateritic profile. Technological characterization studies and selective leaching investigations emphasize that the deportment of Ni and Co strongly influences leachability, Fe co-dissolution, and downstream recovery options (Eljoudiani et al., 2024; Zablotskaya et al., 2020; Zablotskaya et al., 2022).

Kinetic modeling can support process selection, but linearized pseudo-first-order and shrinking-core transformations should be interpreted with caution when early dissolution is rapid and extraction approaches a plateau. The present study follows the diagnostic use of apparent kinetics rather than claiming a single rate-controlling mechanism, consistent with work comparing shrinking-core and lumped models and with critical discussions of kinetic interpretation in ore leaching tests (Wanta et al., 2020; Pereira, 2026a; Wang et al., 2024; Setiawan et al., 2023; Prameswara et al., 2023).

The objective of this work is to transform corrected bench-scale leaching data into an operational decision framework for a ferruginous lateritic nickel ore. The intended contribution is not a definitive statistical optimization, given the limited experimental matrix, but rather a transparent screening method that integrates mineralogy, extraction response, apparent kinetics, Fe

JIRRS
Journal International Review of Research Studies
Received: 02/05/2026 - **Accepted:** 07/07/2026
Vol: 01.09
DOI: 10.66104/dempc459
Pages: 1-30

penalty, acid dosage, and residence time. The study therefore supports a practical operating-window decision and identifies what validation data are required before detailed process design.

2. Materials and Methods

2.1. Ore sample and mineralogical basis

Leaching tests were performed on a fraction of ferruginous lateritic nickel ore retained on a 100-mesh sieve. The initial composition was about 1.08 wt.% Ni, 33.53 wt.% Fe, 2.68 wt.% Mg, 1.86 wt.% Cr, 0.605 wt.% Mn, 0.964 wt.% Al, and 13.32 wt.% Si. The ore was mineralogically interpreted as limonitic, dominated by iron oxyhydroxides and a siliceous–ferruginous matrix called Si–Fe plasma, a fine-grained, poorly crystalline or amorphous siliceous–ferruginous material identified via mineralogy and electron microscopy. Nickel mainly associates with iron oxyhydroxides and Si–Fe plasma, with some in phyllosilicates in the coarser fraction. This distribution explains how aggressive acid leaching improves Ni extraction and promotes Fe dissolution.

The experimental workflow began with the selection of the 100-mesh retained ore fraction, followed by head assay and mineralogical characterization to establish the chemical and mineralogical basis for interpreting the leaching response. Atmospheric sulfuric acid leaching was then conducted at 95–100 °C using acid dosages of 700- 1000 kg H_2SO_4/t ore, with time-series sampling over 30- 420 min. Liquor, wash water, and dry residue assays were used to calculate corrected extraction values via direct mass balance. These corrected data were subsequently applied to apparent kinetic diagnosis and to the development of the acid–Fe–time penalty index, P, which supports the selection of operating conditions that balance nickel recovery, iron dissolution, acid consumption, and residence time.

The chemical composition of the ore fraction used in the leaching tests is presented in Table 1. The ore is characterized by a low nickel grade and a high iron content, consistent with a ferruginous limonitic laterite. The presence of Mg, Al, Mn, Cr, and Si is also relevant, as these elements may contribute to acid consumption, impurity loading, and downstream solution purification requirements.

Table 1. Initial ore composition used for process interpretation

Element	Head grade (wt.%)	Process relevance
Ni	1.080	Target metal and basis for recovery calculation
Fe	33.530	Dominant impurity and major acid/front-end penalty
Mg	2.680	Acid-consuming gangue component
Cr	1.860	Low-solubility impurity; commonly related to chromite
Mn	0.605	Reactive impurity commonly associated with Mn oxides

JIRRS
Journal International Review of Research Studies
Received: 02/05/2026 - **Accepted:** 07/07/2026
Vol: 01.09
DOI: 10.66104/dempc459
Pages: 1-30

Al	0.964	Gangue impurity relevant to solution purification
Si	13.320	Siliceous component, including Si-Fe plasma and quartz/chalcedony

The head grade of 1.08 wt.% Ni defines the target metal inventory for extraction calculations, whereas the high Fe content (33.53 wt.%) confirms that iron is the dominant impurity and the main front-end process constraint. Magnesium and aluminum are acid-consuming gangue components, whereas manganese may contribute to solution impurity loading, depending on its mineralogical association and dissolution behavior. Silicon is mainly associated with siliceous phases and the Si–Fe plasma, which may affect both nickel deportment and leaching selectivity. Therefore, the ore composition supports the need for a decision criterion that considers not only nickel recovery, but also Fe dissolution and acid intensity

To strengthen the mineralogical basis used for interpreting the leaching response, Table 2 summarizes the main mineralogical features considered in this study, the evidence supporting their identification, and their process significance. The purpose of this table is not to provide a complete quantitative deportment analysis, but to clarify the mineralogical assumptions that support the observed trade-off between nickel extraction and iron dissolution. In particular, the association of nickel with iron oxyhydroxides and Si–Fe plasma provides a mineralogical explanation for the loss of Ni/Fe selectivity under more severe sulfuric acid leaching conditions.

Table 2. Mineralogical evidence used to support the interpretation of Ni/Fe co-dissolution.

Mineralogical feature	Evidence used in this study	Process interpretation
Iron oxyhydroxides/goethite-limonite	Dominant ferruginous matrix inferred from chemical composition and mineralogical characterization	Main Fe-rich host environment; acid attack can release Ni while dissolving Fe.
Si-Fe plasma	Fine-grained poorly crystalline to amorphous siliceous-ferruginous matrix observed by automated mineralogy/electron microscopy	Supports coupled Ni extraction and Fe dissolution, especially at higher acid severity.
Subordinate phyllosilicates	Minor contribution in the coarse retained fraction	May contribute to early Ni release and Mg/Si-bearing solution load.
Chromite/quartz/chalcedony and resistant silicates	Inferred from Cr and Si inventories and mineralogical observations	Expected to remain comparatively less reactive under the tested atmospheric conditions.
Ni deportment	Qualitatively classified as mainly associated with Fe oxyhydroxides and Si-Fe plasma, with subordinate phyllosilicates	Explains why higher Ni extraction is accompanied by Fe co-dissolution and loss of selectivity.

Note. The table provides a concise mineralogical basis for the screening interpretation. It is not a complete modal mineralogy or quantitative deportment table; detailed mineralogical outputs should be supplied as supplementary evidence where available.

Figure 1 summarizes the experimental and decision workflow adopted in this study. The procedure started with the selection of the 100-mesh retained ore fraction, followed by head assay

JIRRS
Journal International Review of Research Studies
Received: 02/05/2026 - **Accepted:** 07/07/2026
Vol: 01.09
DOI: 10.66104/dempc459
Pages: 1-30

and mineralogical characterization. Atmospheric sulfuric acid leaching was then performed at 95–100 °C using acid dosages of 700- 1000 kg H_2SO_4/t ore, with time-series sampling over 30- 420 min. Liquor, wash water, and dry residue assays were used to calculate corrected extraction values via direct mass balance. These data were subsequently applied to apparent kinetic diagnosis and to the acid–Fe–time penalty index, P, which was used to support the selection of a practical operating window.

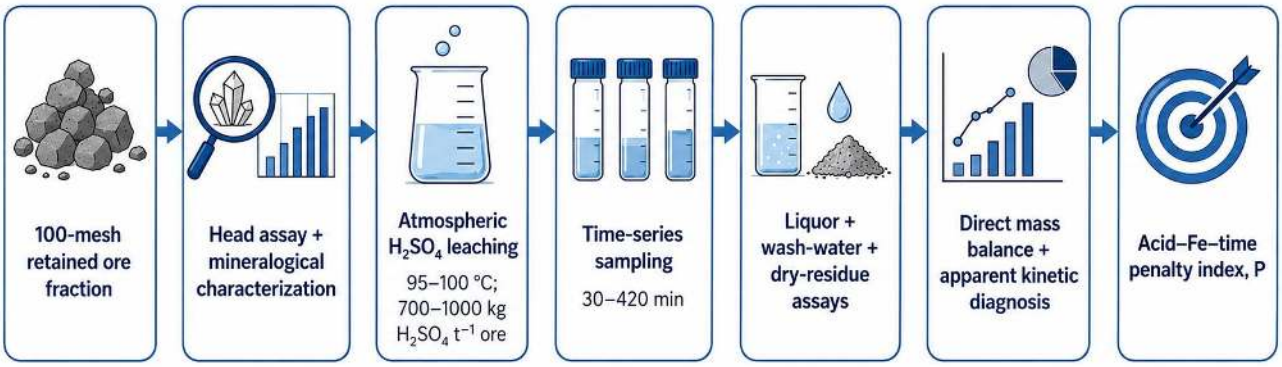

Figure 1. Experimental and decision workflow used to convert leaching test data into an operational screening criterion.

2.2. Leaching tests

The atmospheric sulfuric acid leaching tests were designed to evaluate the effect of acid dosage under a constant initial slurry basis, as summarized in Table 3. Four tests were conducted using 600 g of ore in each experiment, with the total initial slurry mass fixed at 3000 g. The sulfuric acid dosage was varied from 700 to 1000 kg H_2SO_4/t ore by adjusting the relative masses of acid and water added to the slurry, while maintaining the same ore mass and initial slurry mass in all tests. The reaction temperature was maintained at approximately 95–100 °C, and time-series samples were collected between 30 and 420 min. The tests were coded as R700, R800, R900, and R1000 according to the nominal sulfuric acid dosage.

Table 3. Atmospheric sulfuric acid leaching test conditions.

Test	Ore (g)	H_2SO_4 (g)	Water (g)	Initial slurry (g)	Acid dosage (kg H_2SO_4/t ore)
R700	600	420	1980	3000	700
R800	600	480	1920	3000	800
R900	600	540	1860	3000	900
R1000	600	600	1800	3000	1000

The constant ore mass and initial slurry mass allowed the effect of acid dosage to be isolated from changes in the initial slurry basis. As the sulfuric acid addition increased from R700 to R1000, the water addition was proportionally reduced to maintain a total initial slurry mass of 3000 g in all tests. This approach ensured that differences in nickel extraction and iron dissolution could be

JIRRS
Journal International Review of Research Studies
Received: 02/05/2026 - **Accepted:** 07/07/2026
Vol: 01.09
DOI: 10.66104/dempc459
Pages: 1-30

primarily attributed to acid dosage and residence time, rather than to variations in initial pulp dilution.

2.3. Analytical methods and QA/QC

Liquor and wash solutions were analyzed for dissolved metals, and residues were dried and analyzed chemically. The calculation procedure used paired solution and residue data to minimize reliance on a single stream. Values below the analytical quantification limit were treated conservatively, using the reported limit when required for mass-balance calculations. Duplicate data available in the analytical certificates were used as a qualitative check on residue heterogeneity. Non-monotonic behavior in Fe and other elements was not smoothed; instead, it was retained and discussed as part of the data-quality interpretation. The R1000 values from 240 to 420 min were retained only after direct recalculation from measured liquor, wash-water, and dry-residue data, and are explicitly identified as corrected/recalculated values.

The study is interpreted as an operational screening exercise. It does not replace replicate testing, independent inter-laboratory QA/QC, or a formal design-of-experiments optimization. Before detailed engineering, the selected condition should be repeated, the full liquid-solid mass balance should be independently closed, and raw analytical uncertainty should be propagated through the extraction and penalty calculations.

2.4. Extraction calculation and corrected mass balance

Element extraction was calculated from soluble mass in the pregnant leach solution and wash water relative to the sum of soluble and residual masses. The calculation basis was:

(1) $m_{soluble,i} = C_{liquor,i} \times V_{liquor} + C_{wash,i} \times V_{wash}$

(2) $m_{residue,i} = (G_{residue,i} / 100)\, m_{dry\ residue}$

(3) $X_i = [m_{soluble,i} / (m_{soluble,i} + m_{residue,i})] \times 100$

where C is the measured concentration, V is the corresponding solution volume, $G_{residue,i}$ is the dry-residue grade of element i, m_dry residue is the dry residue mass, and X_i is the extraction or dissolution of element i. Equations (1)-(3) were applied consistently to Ni, Fe, and the other reported elements.

The original spreadsheet for the R1000 test contained inconsistent formula-based values at longer times. Rather than excluding the longer residence times, the 240-420 min data were retained

JIRRS
Journal International Review of Research Studies
Received: 02/05/2026 - **Accepted:** 07/07/2026
Vol: 01.09
DOI: 10.66104/dempc459
Pages: 1-30

after recalculation by direct balance using measured liquor, wash-water, and dry-residue data. These values are used to evaluate whether excessive acid dosage offers a process advantage.

2.5. Apparent kinetic modeling

Three apparent kinetic transformations were tested as comparative diagnostic tools. Because the first sampling point already showed substantial extraction, the regressions were performed with intercept a rather than being forced through the origin. The transformations were:

(4) pseudo-first-order: $-\ln(1 - X) = a + k_{app} \times t$

(5) shrinking-core reaction control: $1 - (1 - X)^{(1/3)} = a + k_{app} \times t$

(6) shrinking-core product-layer diffusion control: $1 - 3(1 - X)^{(2/3)} + 2(1 - X) = a + k_{app} \times t$

(7) kinetic selectivity: $S_k = k_{Ni} / k_{Fe}$

In Equations (4)-(7), X is the fractional extraction or dissolution, t is the leaching time in minutes, k_{app} is the apparent rate constant, and S_k is the ratio between apparent nickel and iron dissolution rates. These equations were used for ranking and diagnosis only; high R^2 values were not interpreted as proof of a unique rate-controlling mechanism.

2.6. Decision index and acceptance limits

The decision framework uses an acceptance filter followed by a penalty ranking. The acceptance filter requires Ni extraction of at least 80% and Fe dissolution of no more than 50%. These values are practical screening limits for this ore and this early-stage front-end design problem. The 80% Ni limit represents a minimum recovery threshold sufficient to compare acid dosage and residence time without forcing maximum extraction. The 50% Fe limit reflects the need to avoid excessive Fe loading in the pregnant leach solution, which would increase acid consumption, neutralization demand, solid generation, and impurity-removal burden. These limits are not universal and should be redefined for a specific flowsheet, economic model, and downstream Fe-removal capacity.

The acid-Fe-time penalty index was defined as:

(8) $P = (M_{Fe} / M_{Ni}) \times (D / D_{ref}) \times (t / t_{ref})$

where M_{Fe}/M_{Ni} is the dissolved Fe-to-recovered Ni mass ratio, D is acid dosage in kg H_2SO_4/t ore, t is residence time in minutes, D_{ref} = 800 kg H_2SO_4/t ore, and t_{ref} = 300 min. These reference values represent the central practical candidate in the experimental matrix, not an independently optimized plant target. Lower P indicates a lower Fe burden per unit Ni recovered,

JIRRS
Journal International Review of Research Studies
Received: 02/05/2026 - **Accepted:** 07/07/2026
Vol: 01.09
DOI: 10.66104/dempc459
Pages: 1-30

lower acid intensity, and shorter residence time. Alternative D_{ref} and t_{ref} values only rescale P by a constant factor and therefore do not change ranking, provided that the same references are applied to all conditions.

Threshold sensitivity was evaluated by testing stricter Ni and Fe acceptance limits and by rescaling the penalty index with alternative reference values. This sensitivity analysis was used to check whether the selected point was an artifact of the chosen screening limits or of the numerical references in Equation (8).

3. Results and Discussion

3.1. Corrected extraction database

Table 4 summarizes the corrected extraction values for the complete set of elements. The decision framework focuses on Ni recovery and Fe dissolution because Fe is the major acid-consuming and front-end-impacting impurity, but Co, Mg, Mn, Zn, Al, Cr, Cu, and Si were retained to maintain transparency of the chemical response.

Fe was selected as the primary penalty term because it dominates the mass loading of the leach liquor for this ferruginous ore and directly affects acid consumption, neutralization demand, Fe-rich precipitate generation, impurity removal, and solid-liquid separation. Mg, Al, Mn, Co, Zn, Cr, Cu, and Si are nevertheless reported to preserve chemical transparency. Future versions of the index may include a broader impurity- or neutralization-load term, such as Mg + Al + Mn or total acid-consuming cations, if downstream data indicate that these species govern purification cost or residue generation.

Table 4. Corrected extraction values used in the revised interpretation

R (kg H_2SO_4/t ore)	Time (min)	Al (%)	Co (%)	Cr (%)	Cu (%)	Fe (%)	Mg (%)	Mn (%)	Ni (%)	Si (%)	Zn (%)
700.0	30.0	45.4	18.3	2.2	37.8	26.4	79.2	15.8	47.2	0.4	39.2
700.0	60.0	49.0	23.1	2.6	20.1	31.1	79.6	19.5	52.9	0.3	44.1
700.0	120.0	48.3	27.2	2.8	22.1	32.5	79.7	22.6	56.2	0.4	47.2
700.0	240.0	57.5	40.0	3.8	30.1	40.6	96.8	31.9	71.8	0.4	60.0
700.0	300.0	55.4	45.0	4.1	32.8	40.6	97.4	35.4	74.1	0.4	61.8
700.0	360.0	53.4	48.6	4.8	33.8	39.3	98.9	38.1	76.4	0.4	63.7
700.0	420.0	58.1	59.7	16.3	47.0	49.1	100.0	41.8	84.9	0.1	70.9
800.0	30.0	46.3	20.5	2.5	21.0	30.0	77.0	17.9	50.4	0.3	42.2
800.0	60.0	49.9	25.2	3.0	22.9	36.6	76.9	21.7	56.0	0.3	47.9
800.0	120.0	48.4	31.4	3.4	26.8	39.5	81.7	26.5	62.7	0.3	54.1
800.0	240.0	56.8	44.5	4.3	34.6	49.1	96.9	36.7	78.6	0.3	67.6
800.0	300.0	55.2	49.5	4.5	36.8	48.4	100.0	39.6	82.8	0.3	71.4
800.0	360.0	52.1	53.1	5.1	37.6	45.2	100.0	42.3	83.7	0.4	71.9
800.0	420.0	54.3	61.5	12.6	48.5	51.7	100.0	41.8	89.3	0.1	76.2
900.0	30.0	46.9	22.0	2.7	21.2	32.2	74.9	19.3	52.3	0.2	44.8

JIRRS
Journal International Review of Research Studies
Received: 02/05/2026 - **Accepted:** 07/07/2026
Vol: 01.09
DOI: 10.66104/dempc459
Pages: 1-30

900.0	60.0	47.6	25.4	3.1	24.0	37.4	72.3	22.3	55.5	0.2	48.5
900.0	120.0	53.1	35.8	3.8	31.4	44.1	82.2	30.7	69.0	0.2	61.1
900.0	240.0	51.6	43.2	4.2	34.0	47.6	85.9	36.2	74.5	0.3	66.3
900.0	300.0	51.2	50.7	4.7	37.8	46.8	93.4	41.9	82.4	0.3	73.1
900.0	360.0	54.7	58.0	5.3	41.4	52.2	100.0	46.8	89.9	0.3	79.4
900.0	420.0	57.5	67.5	12.4	48.4	57.7	100.0	47.7	91.0	0.1	83.4
1000.0	30.0	51.5	26.3	3.3	26.5	40.1	76.4	23.5	59.1	0.1	51.6
1000.0	60.0	47.7	28.0	3.4	26.0	40.4	69.4	24.6	57.0	0.1	50.9
1000.0	120.0	53.4	38.7	4.5	33.3	50.9	79.8	33.1	70.6	0.1	63.6
1000.0	240.0	54.8	32.9	6.7	39.2	71.3	84.9	29.6	83.1	0.1	76.9
1000.0	300.0	62.9	46.0	7.8	47.0	78.1	90.7	42.0	88.1	0.1	82.2
1000.0	360.0	62.5	43.8	8.1	46.2	80.2	90.0	39.9	89.1	0.1	83.0
1000.0	420.0	61.2	47.0	8.3	47.3	80.4	90.8	42.1	89.5	0.1	82.5

The corrected extraction database was used to compare the effect of acid dosage and residence time on nickel extraction and iron dissolution. Figure 2 shows that nickel extraction generally increased with increasing leaching time and acid dosage, whereas iron dissolution also increased, particularly under more aggressive acid conditions. The horizontal reference lines at 80% Ni extraction and 50% Fe dissolution represent the practical screening limits adopted in this study to identify conditions that provide acceptable nickel recovery without excessive iron solubilization.

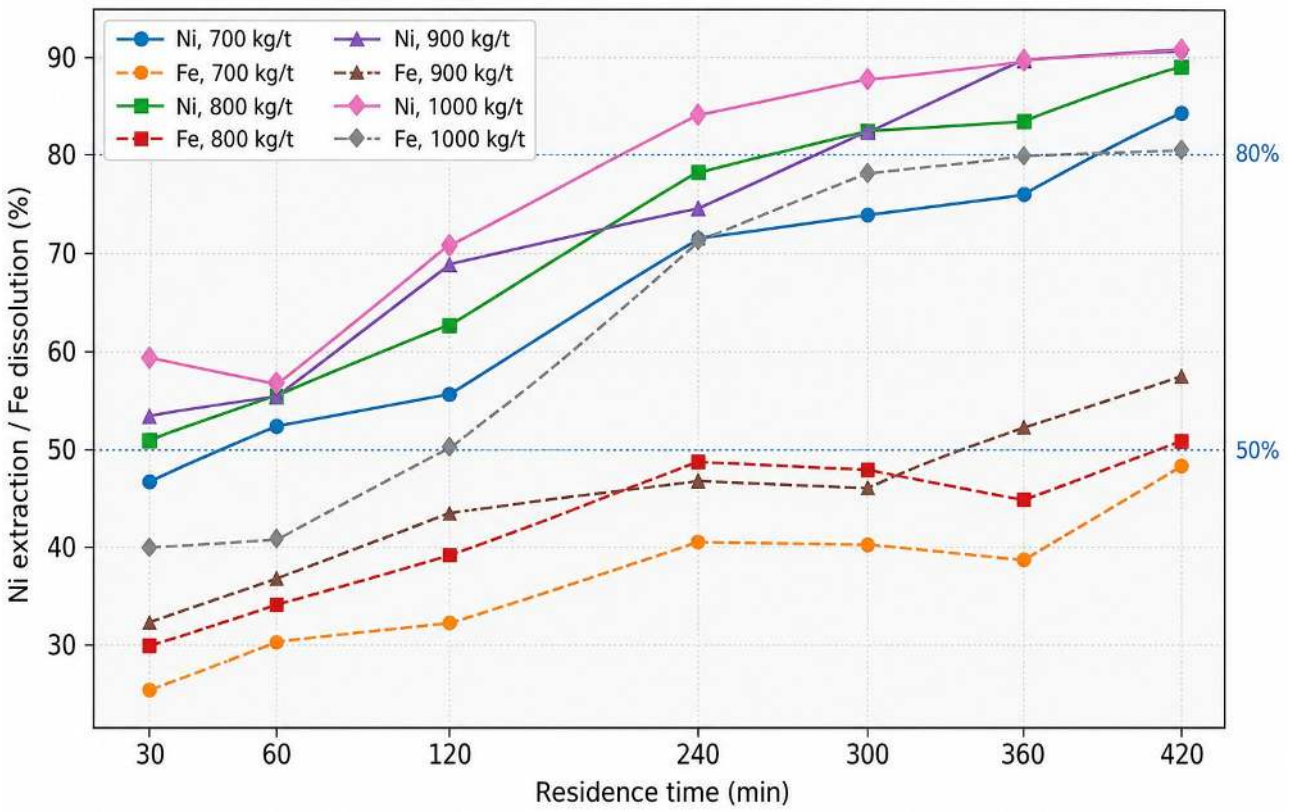

Figure 2. Nickel extraction and iron dissolution as functions of residence time and acid dosage. Horizontal reference lines indicate Ni = 80% and Fe = 50%.

JIRRS
Journal International Review of Research Studies
Received: 02/05/2026 - **Accepted:** 07/07/2026
Vol: 01.09
DOI: 10.66104/dempc459
Pages: 1-30

The results confirm the strong trade-off between nickel recovery and iron dissolution. At 700 kg H_2SO_4/t ore, nickel extraction increased progressively with residence time, reaching the acceptable region only at 420 min, when Ni extraction was approximately 84.9%, and Fe dissolution remained close to the 50% limit. At 800 kg H_2SO_4/t ore, the system reached a more favorable compromise, achieving 82.8% Ni extraction at 300 min while keeping Fe dissolution below the adopted threshold. Increasing the acid dosage to 900 kg/t improved nickel extraction at longer residence times, but Fe dissolution exceeded the preferred limit after 360 min. The 1000 kg/t condition yielded high nickel extraction but also caused severe iron dissolution, particularly between 240 and 420 min, indicating poor Ni/Fe selectivity. Therefore, the graphical response supports selecting 800 kg H_2SO_4/t ore and 300 min as the most balanced operating condition within the tested experimental range.

3.2. Effect of retaining the R1000 data from 240 to 420 min

Retaining the corrected R1000 data from 240 to 420 min strengthens the process interpretation by allowing evaluation of the highest-acid condition rather than excluding it. These recalculated values show that using 1000 kg H_2SO_4/t ore increased nickel extraction but also caused excessive iron dissolution. At 240 min, the R1000 test already achieved 83.1% Ni extraction, but Fe dissolution reached 71.3%. At 420 min, Ni extraction increased to approximately 89.5%, while Fe dissolution rose to 80.4%.

The corrected and recalculated results for the R1000 test are summarized in Table 5. These values correspond to the longer residence times and were obtained by direct mass-balance recalculation using measured data on liquor, wash water, and dry residue. Their inclusion demonstrates that the highest acid dosage does not confer a meaningful advantage over the 800–900 kg/t conditions in terms of nickel recovery. Instead, it imposes a severe Fe penalty, increases the dissolved Fe/Ni ratio, and raises the overall process penalty. Therefore, the R1000 condition is retained in the analysis as evidence of the limited benefit and poor selectivity associated with excessive acid addition.

Table 5. Corrected and recalculated extraction values retained for the R1000 atmospheric sulfuric acid leaching test.

Time (min)	Ni (%)	Co (%)	Fe (%)	Mg (%)	Mn (%)	Zn (%)	Fe/Ni (kg/kg)	P
240.00	83.1	32.9	71.3	84.9	29.6	76.9	26.6	26.64
300.00	88.1	46.0	78.1	90.7	42.0	82.2	27.5	34.40
360.00	89.1	43.8	80.2	90.0	39.9	83.0	27.9	41.92
420.00	89.5	47.0	80.4	90.8	42.1	82.5	27.9	48.81

Source: Authors' calculations from corrected mass-balance calculations based on liquor, wash-water, and dry-residue analytical data

JIRRS
Journal International Review of Research Studies
Received: 02/05/2026 - **Accepted:** 07/07/2026
Vol: 01.09
DOI: 10.66104/dempc459
Pages: 1-30

The R1000 condition achieved high nickel extraction, from 83.1% at 240 min to 89.5% at 420 min, but also caused severe iron dissolution, reaching 80.4% at 420 min. The Fe/Ni ratio stayed high, between 26.6 and 27.9 kg/kg, and the penalty index rose from 26.64 to 48.81. These results show that high acid dosage led to non-selective dissolution and was not a favorable process, despite the high nickel extraction. R1000 is noted as an example of the penalties of excessive acid.

The downstream penalty associated with excessive acid dosage was further quantified by comparing the selected condition, R800/300, with the most severe high-acid condition, R1000/420, as shown in Table 6. At R800/300, approximately 162.3 kg Fe/t ore and 8.94 kg Ni/t ore entered solution, yielding 18.15 kg of dissolved Fe per kg of recovered Ni. At R1000/420, approximately 269.6 kg Fe/t ore and 9.67 kg Ni/t ore entered solution, giving 27.9 kg Fe/kg Ni. Therefore, increasing severity from R800/300 to R1000/420 added about 107 kg Fe/t ore for only about 0.72 kg additional Ni/t ore. This corresponds to roughly 149 kg of extra Fe dissolved per additional kilogram of Ni recovered, which explains why R1000/420 is not a favorable front-end option.

Table 6. Quantification of the R1000 Fe penalty relative to the selected screening condition.

Condition	Ni extraction (%)	Fe dissolution (%)	Ni dissolved (kg/t ore)	Fe dissolved (kg/t ore)	Fe/Ni (kg/kg)	Interpretation
R800/300	82.8	48.4	8.94	162.3	18.15	Selected the lowest-penalty acceptable condition
R1000/420	89.5	80.4	9.67	269.6	27.9	High Ni but severe Fe penalty
Difference	+6.7 p.p.	+32.0 p.p.	+0.72	+107.3	+9.75	About 149 kg extra Fe per kg additional Ni

3.3. Apparent kinetics and kinetic selectivity

Apparent kinetic modeling was retained as a comparative diagnostic tool to assess the effects of sulfuric acid dosage on the relative dissolution behavior of nickel and iron. Table 7 summarizes the apparent rate constants, standard errors, coefficients of determination, and kinetic selectivity indices (maiúscula S inferior à linha k) obtained from the pseudo-first-order, shrinking-core reaction-control, and shrinking-core diffusion-control transformations. The kinetic selectivity index was calculated as the ratio between the apparent nickel and iron dissolution rate constants, with higher values indicating more favorable Ni dissolution relative to Fe.

The results show that the R800 condition provides the strongest Ni/Fe kinetic selectivity among the 700–900 kg H_2SO_4/t ore tests. This trend is consistent across the evaluated kinetic transformations, indicating that 800 kg H_2SO_4/t ore offers the most favorable apparent kinetic

JIRRS
Journal International Review of Research Studies
Received: 02/05/2026 - **Accepted:** 07/07/2026
Vol: 01.09
DOI: 10.66104/dempc459
Pages: 1-30

compromise between nickel extraction and iron dissolution. In contrast, the R1000 condition approaches non-selective behavior, with S_k values close to unity, because Fe dissolves at a rate comparable to that of Ni. Therefore, the kinetic analysis supports rejecting excessive acid dosage and reinforces the selection of R800 as the most balanced condition within the tested range.

Table 7. Apparent kinetic constants, standard errors, and kinetic selectivity

R (kg/t)	Model	k_Ni (min^{-1})	SE k_Ni	R^2 Ni	k_Fe (min^{-1})	SE k_Fe	R^2 Fe	S_k
700	Pseudo-first-order	2.90E-03	2.60E-04	0.96	7.57E-04	1.27E-04	0.88	3.83
700	SCM reaction-control	6.52E-04	4.74E-05	0.97	2.15E-04	3.52E-05	0.88	3.03
700	SCM diffusion-control	8.31E-04	7.28E-05	0.96	1.60E-04	2.98E-05	0.85	5.18
800	Pseudo-first-order	3.79E-03	2.02E-04	0.99	8.03E-04	1.67E-04	0.82	4.72
800	SCM reaction-control	7.95E-04	4.24E-05	0.99	2.23E-04	4.68E-05	0.82	3.56
800	SCM diffusion-control	1.07E-03	5.48E-05	0.99	1.84E-04	3.80E-05	0.82	5.81
900	Pseudo-first-order	4.32E-03	4.01E-04	0.96	1.00E-03	1.34E-04	0.92	4.32
900	SCM reaction-control	8.67E-04	6.65E-05	0.97	2.71E-04	3.64E-05	0.92	3.20
900	SCM diffusion-control	1.19E-03	1.01E-04	0.97	2.43E-04	3.35E-05	0.91	4.89
1000	Pseudo-first-order	4.02E-03	3.61E-04	0.96	3.32E-03	2.89E-04	0.96	1.21
1000	SCM reaction-control	8.02E-04	8.24E-05	0.95	7.79E-04	7.29E-05	0.96	1.03
1000	SCM diffusion-control	1.12E-03	1.07E-04	0.96	9.37E-04	8.23E-05	0.96	1.19

The apparent kinetic results confirm that acid dosage strongly influenced Ni/Fe selectivity. Among the 700–900 kg H_2SO_4/t ore tests, the 800 kg/t condition showed the most favorable kinetic response. In the pseudo-first-order model, R800 presented the highest kinetic selectivity, with $S_k = 4.72$, compared with $S_k = 3.83$ for R700 and $S_k = 4.32$ for R900. The same trend was reinforced by the SCM diffusion-control transformation, for which R800 reached the highest selectivity value, $S_k = 5.81$.

In contrast, the R1000 condition showed very poor kinetic selectivity in all transformations, with S_k values close to unity. This indicates that, under the highest acid dosage, Fe dissolution proceeded almost as rapidly as Ni dissolution. Therefore, increasing the acid dosage to 1000 kg H_2SO_4/t ore did not improve the process selectivity; instead, it promoted non-selective dissolution. These results support the interpretation that R800 provides the best kinetic compromise among the evaluated acid dosages, whereas R1000 should be rejected because of its excessive Fe dissolution and low Ni/Fe kinetic selectivity.

JIRRS
Journal International Review of Research Studies
Received: 02/05/2026 - **Accepted:** 07/07/2026
Vol: 01.09
DOI: 10.66104/dempc459
Pages: 1-30

To complement the extraction-based interpretation, an apparent kinetic selectivity index was calculated as the ratio between the apparent nickel and iron dissolution rate constants. Figure 3 compares the pseudo-first-order kinetic selectivity index, $S_k = k_{Ni}/k_{Fe}$, for the four acid dosages evaluated. This index was used only as a comparative diagnostic parameter, with higher values indicating more favorable kinetic separation between nickel extraction and iron dissolution.

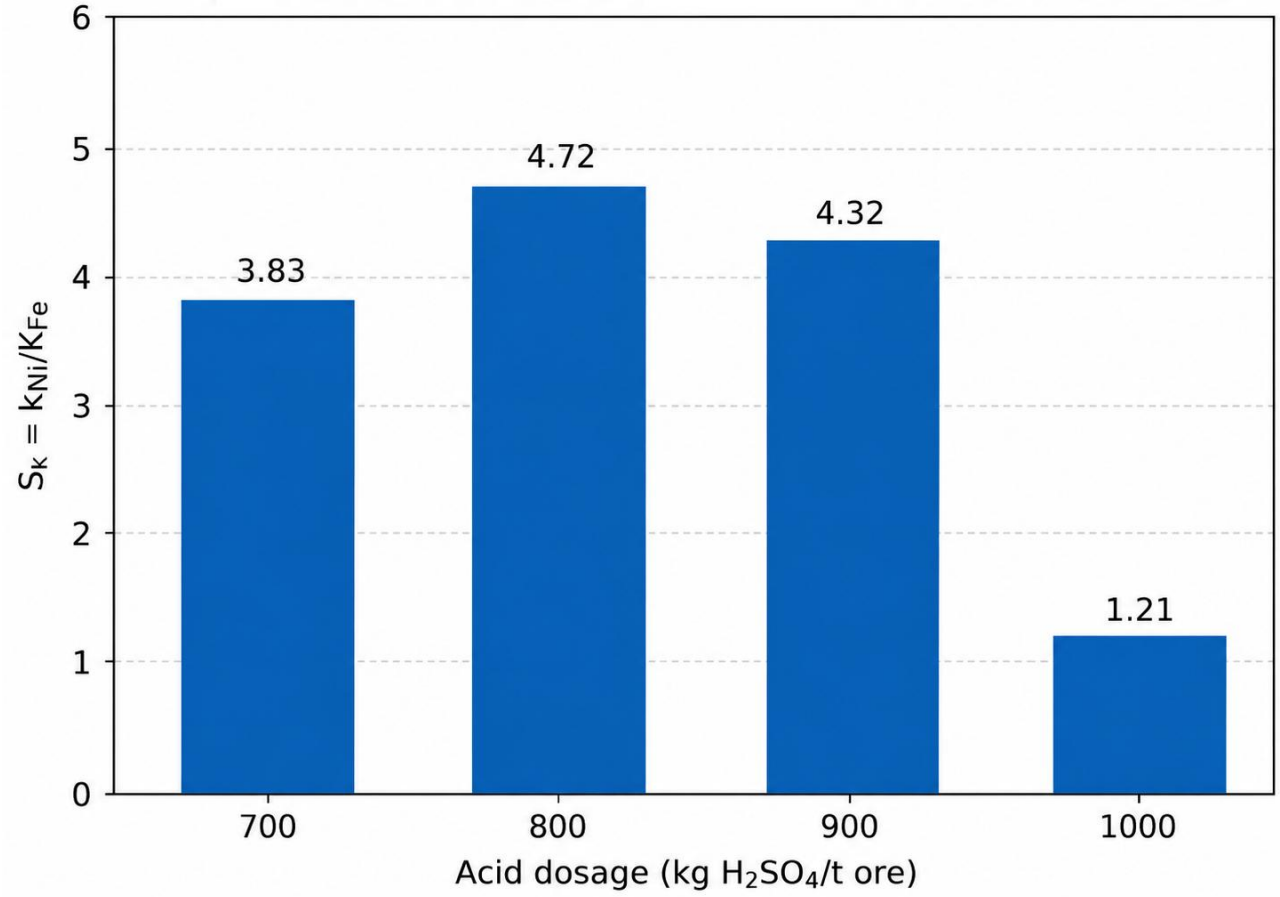

Figure 3. Apparent kinetic selectivity index from pseudo-first-order fits. R800 gives the highest Ni/Fe selectivity among 700-900 kg/t, while R1000 shows poor selectivity.

The corrected kinetic results support the process decision but require a more cautious interpretation than a fixed threshold such as $S_k >= 5$. The R800 condition gives the highest pseudo-first-order kinetic selectivity among the 700-900 kg/t tests, with $S_k = 4.72$. Under the SCM diffusion transformation, the same condition gives $S_k = 5.81$. The R1000 condition gives S_k close to unity in all transformations, confirming that excessive acid dosage accelerates Fe dissolution and erodes Ni/Fe selectivity.

The kinetic regressions were not forced through the origin because the first samples already captured rapid initial dissolution. Forcing zero intercepts would attribute the unobserved early-stage dissolution path to the fitted rate constant, potentially biasing comparisons among acid dosages. In

JIRRS
Journal International Review of Research Studies
Received: 02/05/2026 - **Accepted:** 07/07/2026
Vol: 01.09
DOI: 10.66104/dempc459
Pages: 1-30

addition, R^2 was used only as a goodness-of-fit descriptor; similar R^2 values across transformations do not discriminate a unique mechanism. The extraction curves are therefore interpreted as composite apparent kinetics affected by mineralogical heterogeneity, rapid dissolution of more reactive Ni-bearing domains, Fe co-dissolution, and possible secondary Fe redistribution.

3.4. Decision map and process selection

The corrected extraction values were further interpreted using a decision map linking nickel extraction to iron dissolution. The acceptable region was defined by two practical screening limits: Ni extraction $\geq$ 80% and Fe dissolution $\leq$ 50%. These thresholds are not intended as universal criteria but rather as process-oriented limits for this specific ferruginous lateritic ore and for a front-end leaching route in which Fe dissolution is a major cost, impurity, and burden on downstream treatment.

Figure 4 shows the position of each experimental condition based on its nickel extraction and iron dissolution responses. The horizontal dashed line represents the minimum Ni extraction target, whereas the vertical dashed line indicates the maximum acceptable Fe dissolution. This representation allows the tested conditions to be classified by their ability to achieve sufficient nickel recovery while maintaining controlled iron solubilization. Within the acceptable region, the final selection was based on the condition with the lowest acid–Fe–time penalty index, ensuring that the chosen operating point balances recovery, selectivity, acid dosage, and residence time.

JIRRS
Journal International Review of Research Studies
Received: 02/05/2026 - **Accepted:** 07/07/2026
Vol: 01.09
DOI: 10.66104/dempc459
Pages: 1-30

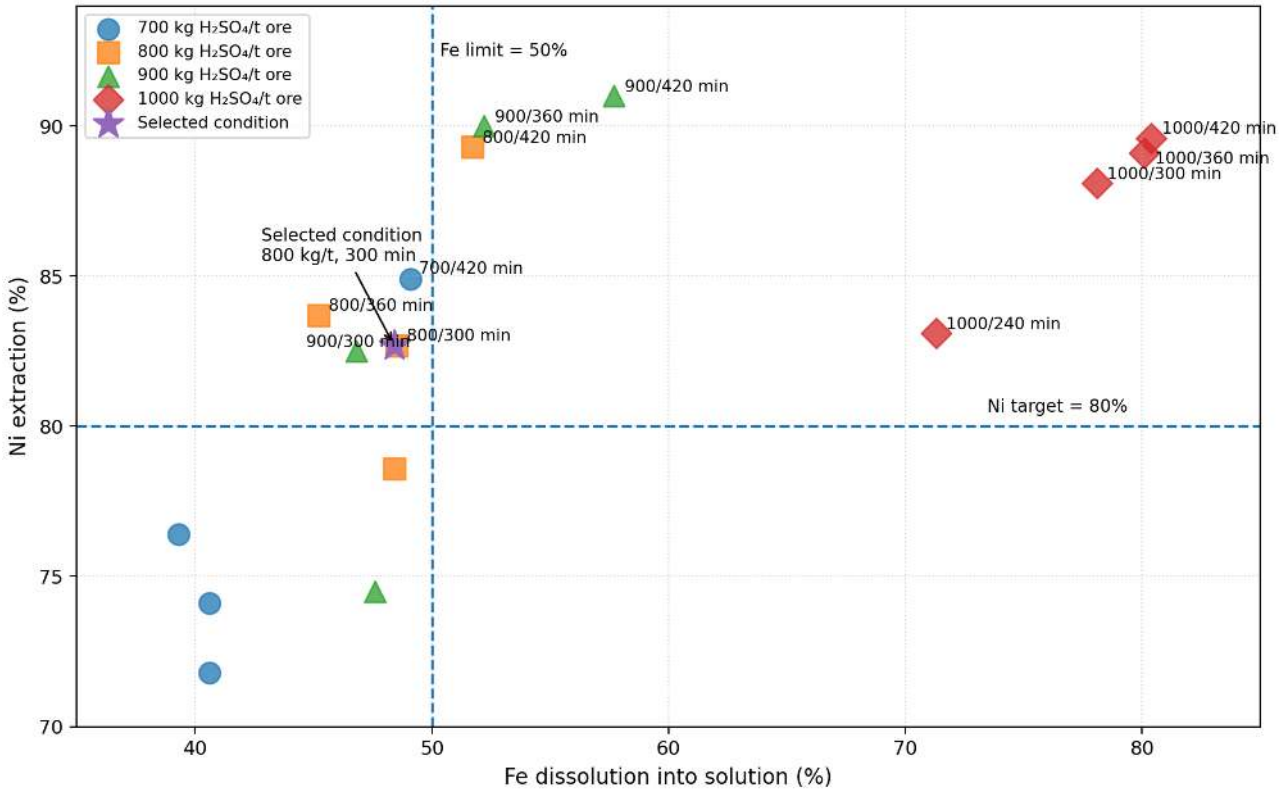

Figure 4. Decision map for Ni extraction versus Fe dissolution. The preferred region is Ni >= 80% and Fe <= 50%; point size reflects residence time. Source: Authors' calculations,

The decision map confirms that process selection should not be based solely on maximizing nickel extraction. The preferred operating region lies above the Ni extraction target and to the left of the Fe dissolution limit. Within this region, 800 kg H_2SO_4/t ore and 300 min provide the most balanced response, achieving approximately 82.8% Ni extraction while keeping Fe dissolution at 48.4%, below the adopted threshold.

The condition of 700 kg/t at 420 min is also technically acceptable, achieving 84.9% Ni extraction and 49.1% Fe dissolution. However, it requires a longer residence time and therefore imposes a higher process penalty than the selected 800 kg/t, 300 min condition. Similarly, 900 kg/t at 300 min meets the acceptance criteria but requires a higher acid dosage and provides no meaningful improvement in Ni extraction relative to the selected condition. In contrast, the higher-severity R1000 conditions are well beyond the Fe dissolution limit, with Fe dissolution exceeding 71% from 240 to 420 min. These results show that excessive acid dosage promotes non-selective dissolution and increases the Fe burden. Therefore, Figure 4 supports the selection of 800 kg H_2SO_4/t ore and 300 min as the most balanced operating point within the tested matrix.

The operating conditions were classified using the combined decision criteria of nickel extraction, iron dissolution, dissolved Fe/Ni mass ratio, and acid–Fe–time penalty index. Table 8

JIRRS
Journal International Review of Research Studies
Received: 02/05/2026 - **Accepted:** 07/07/2026
Vol: 01.09
DOI: 10.66104/dempc459
Pages: 1-30

summarizes the decision matrix after retaining the corrected R1000 data. Conditions were considered acceptable when they achieved Ni extraction ≥ 80% and Fe dissolution ≤ 50%. Among the acceptable conditions, the preferred operating point was selected as the one with the lowest penalty index, P.

Table 8 Decision matrix for atmospheric sulfuric acid leaching conditions after retaining the corrected R1000 data.

Condition	Ni (%)	Fe (%)	Fe/Ni (kg/kg)	P	Status
700 kg/t, 420 min	84.9	49.1	17.9	22.0	Acceptable
800 kg/t, 240 min	78.6	49.1	19.4	15.5	Reject/penalize
800 kg/t, 300 min	82.8	48.4	18.15	18.1	Select
800 kg/t, 360 min	83.7	45.2	16.8	20.1	Acceptable
800 kg/t, 420 min	89.3	51.7	18.0	25.1	Reject/penalize
900 kg/t, 300 min	82.4	46.8	17.6	19.8	Acceptable
900 kg/t, 360 min	89.9	52.2	18.0	24.3	Reject/penalize
900 kg/t, 420 min	91.0	57.7	19.7	31.0	Reject/penalize
1000 kg/t, 240 min	83.1	71.3	26.6	26.6	Reject/penalize
1000 kg/t, 300 min	88.1	78.1	27.5	34.4	Reject/penalize
1000 kg/t, 420 min	89.5	80.4	27.9	48.8	Reject/penalize

Source: Authors' calculations

The decision matrix confirms that 800 kg H_2SO_4/t ore and 300 min are the selected conditions because they satisfy both acceptance criteria and yield the lowest penalty index among the acceptable operating points. These conditions achieved 82.8% Ni extraction, 48.4% Fe dissolution, a dissolved Fe/Ni ratio of 18.15 kg/kg, and a penalty index of P = 18.1.

The condition 700 kg/t at 420 min was also acceptable, but its longer residence time increased the penalty index to P = 22.0. The condition 800 kg/t at 360 min met the Ni and Fe criteria but provided only limited improvement in nickel extraction relative to the selected condition, while increasing residence time. Likewise, 900 kg/t at 300 min was technically acceptable but required a higher acid dosage without improving nickel extraction.

Higher-severity conditions were rejected or penalized for exceeding Fe dissolution limits, missing Ni targets, or high penalties. The R1000 conditions, despite high Ni extraction, had Fe dissolution of 71.3%–80.4%, leading to high Fe/Ni ratios and penalties. The decision matrix shows that the chosen condition is not the one with maximum recovery but the most balanced operating window.

The acid–Fe–time penalty index was used to rank the operating conditions that met or approached the practical screening limits, as shown in Figure 5. Lower values of P *indicate* a more favorable balance between dissolved Fe burden, acid dosage, and residence time. Although several conditions achieved acceptable or near-acceptable nickel extraction, their process penalties differed

JIRRS
Journal International Review of Research Studies
Received: 02/05/2026 - **Accepted:** 07/07/2026
Vol: 01.09
DOI: 10.66104/dempc459
Pages: 1-30

substantially. The selected condition, R800/300, presented the lowest penalty index among the acceptable candidates, with $P = 18.1$. This confirms that the selected operating point was not chosen to maximize nickel extraction, but to provide the most favorable compromise among nickel recovery, iron dissolution, acid intensity, and leaching time.

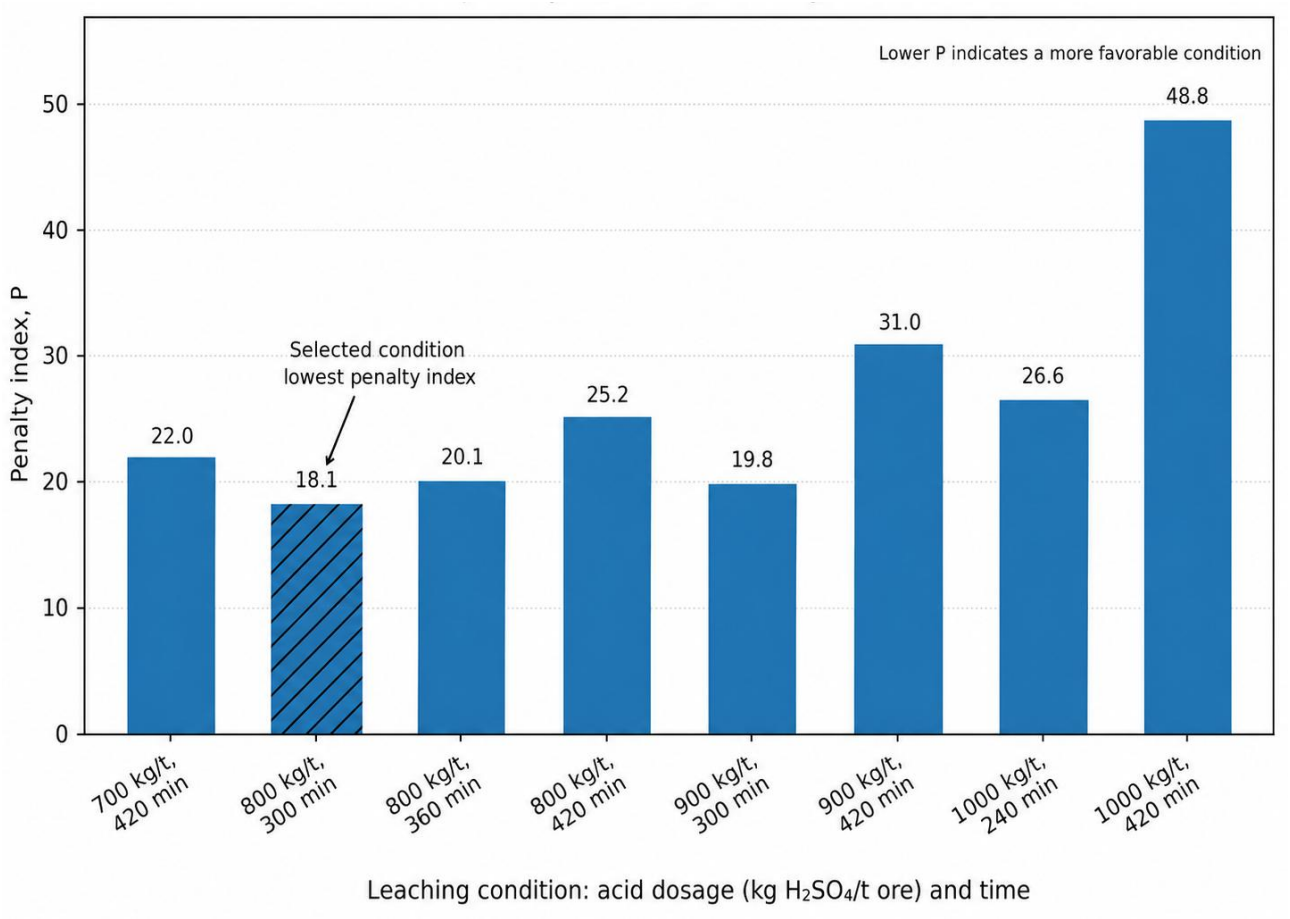

Figure 5. Acid-Fe-time penalty index for selected operating conditions. Lower P indicates a better balance between Fe burden, acid dosage, and residence time.

The penalty ranking confirms that 800 kg H_2SO_4/t ore and 300 min represent the most favorable operating compromise among the evaluated conditions. This point achieved 82.8% Ni extraction while maintaining Fe dissolution at 48.4%, thereby satisfying both the recovery target and the Fe constraint. Its penalty index, P = 18.1, was the lowest among the acceptable candidates, indicating the best balance between nickel recovery, iron burden, acid dosage, and residence time.

Although the condition of 700 kg/t at 420 min also met the practical Ni and Fe criteria, its longer residence time increased the penalty index to P = 22.0. Likewise, 800 kg/t at 360 min and 900 kg/t at 300 min remained technically acceptable, but their higher penalty values indicate less favorable process performance compared with the selected condition. More severe conditions, particularly 900 kg/t at 420 min and 1000 kg/t at 420 min, showed substantially higher penalties due

JIRRS
Journal International Review of Research Studies
Received: 02/05/2026 - **Accepted:** 07/07/2026
Vol: 01.09
DOI: 10.66104/dempc459
Pages: 1-30

to increased Fe dissolution, higher acid intensity, longer residence time, or a combination of these factors.

Therefore, the selected condition should not be interpreted as the maximum-recovery point, but rather as the lowest-penalty operating window that meets the target Ni extraction and Fe dissolution limits while avoiding unnecessary acid consumption and residence time.

The robustness of the selected operating condition was evaluated through a sensitivity analysis of the acceptance thresholds and penalty-index reference values, as summarized in Table 9. The baseline scenario adopted Ni extraction ≥ 80%, Fe dissolution ≤ 50%, an acid reference dosage of 800 kg H_2SO_4/t ore, and a residence-time reference of 300 min. Under these criteria, R800/300 remained the lowest-penalty acceptable condition. When stricter Fe or Ni limits were imposed, no tested condition simultaneously satisfied both constraints, indicating that additional experiments would be required to define a lower-Fe or higher-Ni operating window. When the Fe limit was relaxed to 55%, additional high-recovery points became feasible, but their penalty indices remained higher than those of R800/300. Rescaling the reference acid dosage or residence time did not alter the ranking because all penalty values were multiplied by a constant factor. Therefore, the sensitivity analysis confirms that the selection of R800/300 is not an artifact of the chosen reference values but results from its favorable balance between Ni recovery, Fe control, acid dosage, and residence time.

Table 9. Sensitivity of screening decision to acceptance thresholds and penalty-index references.

Scenario	Acceptance limits/reference values	Lowest-penalty acceptable condition	Outcome
Baseline	Ni ≥ 80%; Fe ≤ 50%; D_{ref} = 800 kg/t; t_{ref} = 300 min	R800/300	P = 18.1; selected
Stricter Fe	Ni ≥ 80%; Fe ≤ 45%	None	No tested point meets both constraints; additional experiments are needed
Stricter Ni	Ni ≥ 85%; Fe ≤ 50%	None	No tested point meets both constraints; R700/420 is close in Ni but below 85%
Relaxed Fe	Ni ≥ 80%; Fe ≤ 55%	R800/300	Higher-recovery points become feasible, but P remains higher
Reference rescaling 1	D_{ref} = 700 kg/t; t_{ref} = 300 min	R800/300	Ranking unchanged; all P values scaled by a constant
Reference rescaling 2	D_{ref} = 800 kg/t; t_{ref} = 240 min	R800/300	Ranking unchanged; all P values scaled by a constant

3.5. Residence-time sensitivity and marginal recovery gain

JIRRS
Journal International Review of Research Studies
Received: 02/05/2026 - **Accepted:** 07/07/2026
Vol: 01.09
DOI: 10.66104/dempc459
Pages: 1-30

Residence-time sensitivity was evaluated at the selected acid dosage of 800 kg H_2SO_4/t ore to determine whether extending the leaching time produced a meaningful increase in nickel recovery. Figure 6 shows the marginal nickel recovery gain between consecutive residence-time intervals. A reference line of 1 percentage point h^{-1} was adopted as the minimum useful gain to support interpretation of whether additional residence time provides a practical metallurgical benefit.

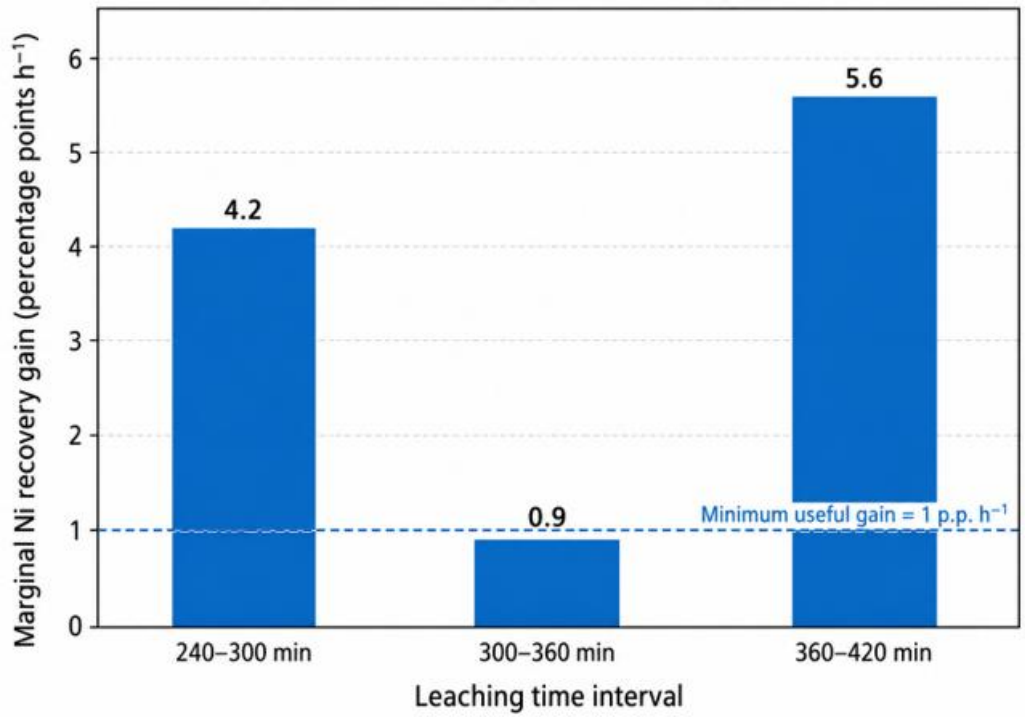

Figure 6. Marginal nickel recovery gain at 800 kg H_2SO_4/t ore. The 420 min point provides additional Ni recovery but fails the Fe constraint and increases the required residence volume. Source: Authors' calculations from corrected nickel extraction values obtained for the R800 atmospheric sulfuric acid leaching test.

The marginal recovery analysis at 800 kg H_2SO_4/t ore indicates that increasing the residence time from 240 to 300 min produced a meaningful improvement in nickel extraction, yielding a gain of 4.2 percentage points h^{-1}. In contrast, extending the leaching time from 300 to 360 min yielded only 0.9 percentage points h^{-1}, which is below the minimum useful gain adopted in this study.

Although the interval from 360 to 420 min showed a higher marginal gain of 5.6 percentage points h^{-1}, this increase came at the cost of selectivity. The corrected final point at 420 min showed 89.3% Ni extraction, while Fe dissolution increased to 51.7%, exceeding the adopted 50% Fe constraint. In addition, for a fixed production rate, increasing the residence time from 300 to 420 min would require approximately 40% more residence volume, heated slurry inventory, and agitation capacity.

JIRRS
Journal International Review of Research Studies
Received: 02/05/2026 - **Accepted:** 07/07/2026
Vol: 01.09
DOI: 10.66104/dempc459
Pages: 1-30

Therefore, the 420 min condition should be considered a higher-recovery alternative only if the downstream process can tolerate the additional Fe load and the larger reactor volume. Under the screening criteria used in this study, the residence-time analysis supports 300 min as the preferred residence time at 800 kg H_2SO_4/t ore because it delivers a meaningful improvement in Ni extraction relative to 240 min while avoiding unnecessary residence time, higher slurry inventory, and excessive Fe dissolution.

3.6. Ternary desirability screening

A ternary desirability diagram was retained as an illustrative screening tool, but the section was streamlined to avoid overextending the interpretation. The diagram integrates three favorable directions: high Ni extraction, low Fe dissolution, and low acid-time intensity. Because the raw variables have different preferred directions, each response was converted to a dimensionless desirability between 0 and 1 before calculating ternary coordinates.

The three desirability components are d_{Ni} for nickel extraction, d_{Fe} for low iron dissolution, and d_{AT} for low acid-time intensity. Acid-time intensity was calculated as:

(9) $IAT = D \times t$

where D is the sulfuric acid dosage in kg H_2SO_4/t ore, and t is the leaching time in minutes. The interpolation domain is restricted to the experimental range $700 \leq D \leq 1000$ kg H_2SO_4/t ore and $240 \leq t \leq 420$ min. Conditions outside this domain should be treated as extrapolations and require additional testing or independent kinetic prediction.

Desirability functions and ternary coordinates

For Ni extraction, which is maximized, the desirability function was defined as:

(10) $d_{Ni} = 0$, if $X_{Ni} < 80\%$

(11) $d_{Ni} = (X_{Ni} - 80)/(82.5 - 80)$, if $80\% \leq X_{Ni} < 82.5\%$

(12) $d_{Ni} = 1$, if $X_{Ni} \geq 82.5\%$

For Fe dissolution, which is minimized, the desirability function was defined as:

(13) $d_{Fe} = 1$, if $X_{Fe} \leq 50\%$

(14) $d_{Fe} = (80 - X_{Fe})/(80 - 50)$, if $50\% < X_{Fe} < 80\%$

(15) $d_{Fe} = 0$, if $X_{Fe} \geq 80\%$

For acid-time intensity, which is also minimized, the desirability function was defined as:

(16) $d_{AT} = 1$, if $I_{AT} \leq 240{,}000$ kg·min/t ore

JIRRS
Journal International Review of Research Studies
Received: 02/05/2026 - **Accepted:** 07/07/2026
Vol: 01.09
DOI: 10.66104/dempc459
Pages: 1-30

(17) $d_{AT} = (420{,}000 - I_{AT})/(420{,}000 - 240{,}000)$, if $240{,}000 < I_{AT} < 420{,}000$ kg·min/t ore

(18) $d_{AT} = 0$, if $I_{AT} \geq 420{,}000$ kg·min/t ore

The lower acid-time reference, 240,000 kg·min/t ore, corresponds to R800/300, while the upper reference, 420,000 kg·min/t ore, corresponds to R1000/420. The normalized ternary coordinates were calculated as:

(19) $T_{Ni} = d_{Ni}/(d_{Ni} + d_{Fe} + d_{AT})$; $T_{Fe} = d_{Fe}/(d_{Ni} + d_{Fe} + d_{AT})$; $T_{AT} = d_{AT}/(d_{Ni} + d_{Fe} + d_{AT})$

and the global desirability index was calculated as:

(20) $D_g = (d_{Ni} \times d_{Fe} \times d_{AT})^{(1/3)}$

where D_g describes the absolute quality of the condition, whereas T_{Ni}, T_{Fe}, and T_{AT} describe the relative balance among the three desirability components. A condition with one desirability equal to zero receives $D_g = 0$ even if the other two responses are favorable.

Worked example: R800/300

For R800/300, $X_{Ni} = 82.8\%$, $X_{Fe} = 48.4\%$, and $I_{AT} = 800 \times 300 = 240{,}000$ kg·min/t ore. Equations (10)-(18) therefore give $d_{Ni} = 1.000$, $d_{Fe} = 1.000$, and $d_{AT} = 1.000$. Equations (19) and (20) then give $T_{Ni} = T_{Fe} = T_{AT} = 0.333$ and $D_g = 1.000$. Thus, R800/300 occupies a balanced position in the ternary diagram and also achieves the highest global desirability among the tested acceptable conditions.

The detailed interpolation example previously shown for 830/270 was removed from the main argument. Intermediate conditions may be estimated only by first interpolating the original metallurgical responses in the acid-dosage/time domain and then recalculating desirability values. The ternary desirability screening was simplified into a concise set of representative experimental and interpolated conditions, as shown in Table 10.

Table 10. Concise desirability table used for ternary screening.

Condition	Ni (%)	Fe (%)	I_{AT} (kg·min/t)	d_{Ni}	d_{Fe}	d_{AT}	D_g	T_{Ni}	T_{Fe}	T_{AT}
700/420	84.9	49.1	294,000	1.000	1.000	0.700	0.888	0.370	0.370	0.259
800/240	78.6	49.1	192,000	0.000	1.000	1.000	0.000	0.000	0.500	0.500
800/300	82.8	48.4	240,000	1.000	1.000	1.000	1.000	0.333	0.333	0.333
800/360	83.7	45.2	288,000	1.000	1.000	0.733	0.902	0.366	0.366	0.268
900/300	82.4	46.8	270,000	0.960	1.000	0.833	0.873	0.344	0.358	0.298
1000/420	89.5	80.4	420,000	1.000	0.000	0.000	0.000	1.000	0.000	0.000
830/270*	81.6	48.0	224,100	0.646	1.000	1.000	0.864	0.244	0.378	0.378

*Interpolated condition. The 830/270 point is included only to illustrate the calculation workflow within the valid interpolation domain; it is not an experimental validation point.

JIRRS
Journal International Review of Research Studies
Received: 02/05/2026 - **Accepted:** 07/07/2026
Vol: 01.09
DOI: 10.66104/dempc459
Pages: 1-30

The desirability results confirm that R800/300 provides the most balanced screening response. Conditions with higher acid dose and longer residence time may increase Ni extraction, but they are penalized by Fe dissolution and acid-time intensity. Conversely, milder or intermediate conditions may achieve favorable Fe control and low operating severity but may fail to meet the Ni extraction target. Therefore, the ternary screening supports R800/300 as the preferred screening condition within the tested and interpolated domain, not as a universal optimum.

The ternary diagram should be interpreted as a visualization of the defined decision logic. It does not replace replicate leaching tests, independent mass-balance closure, uncertainty propagation, or techno-economic optimization.

3.7. Comparison with literature and novelty of the decision framework

The results align with the expected performance of limonitic and ferruginous laterite ores in atmospheric or low-pressure acid leaching. The study's main contribution isn't a new maximum nickel extraction but its novelty in explicitly integrating Ni recovery, Fe dissolution, acid dosage, residence time, and kinetic selectivity into a clear operational screening framework.

This approach differs from studies that focus primarily on maximizing Ni/Co recovery or on fitting leaching kinetics under a fixed process objective (Hosseini Nasab et al., 2020; Santos et al., 2021; Astuti et al., 2024; Prameswara et al., 2023; Prasetya et al., 2025; Ribeiro et al., 2025). In the present study, leaching performance is evaluated from a broader process perspective, in which higher extraction is weighed against impurity dissolution, reagent intensity, and residence-time requirements.

This study compares results with previous research on the processing of lateritic nickel ore, focusing on atmospheric sulfuric acid leaching, kinetics, mineralogical factors, alternative methods, and impurity control. It isn't meant to find a universal best method or replace established technologies like HPAL, but aims to support decision-making for atmospheric leaching. Table 11 highlights key themes and shows how this work advances the evaluation of ferruginous lateritic nickel ores.

Table 11. Literature positioning and quantitative/process comparison

Literature theme	Representative references cited	How the present study compares
Atmospheric H_2SO_4 leaching and kinetics	Hosseini Nasab et al. (2020); Santos et al. (2021); Safitri et al. (2021); Astuti et al. (2024); Prasetya et al. (2025); Ribeiro et al. (2025); Ma et al. (2026)	Present R800/300 gives 82.8% Ni at 300 min with Fe constrained to 48.4%; higher acid gives higher Ni but higher Fe.
Ore type and mineralogical dependence	Eljoudiani et al. (2024); Jeong et al. (2025); Kang et al. (2026); Zablotskaya et al. (2020, 2022)	Present ore is ferruginous and Ni is associated with Fe oxyhydroxides and Si-Fe plasma, explaining limited Ni/Fe

JIRRS
Journal International Review of Research Studies
Received: 02/05/2026 - **Accepted:** 07/07/2026
Vol: 01.09
DOI: 10.66104/dempc459
Pages: 1-30

		selectivity.
Pre-treatment and alternative routes	Dahani et al. (2020); Ribeiro et al. (2020, 2021); Hariyanto et al. (2023); Prameswara et al. (2024); Li et al. (2023, 2026); Osali et al. (2026); Zhao et al. (2024)	Alternative routes may improve extraction but introduce roasting, ammonia, water-leaching, solvent extraction, or SO_3-recovery complexity.
Hydrometallurgical reviews and route selection	Stanković et al. (2020); Bahfie et al. (2022); Pandey et al. (2023); Chi et al. (2026); Acquah et al. (2026); Abbasi Gharaei et al. (2024)	The present study is positioned as atmospheric-leaching screening, not as a replacement for HPAL or integrated flowsheet evaluation.
Kinetic and modeling cautions	Wanta et al. (2020); Setiawan et al. (2023); Wang et al. (2024); Tyassena et al. (2026); Pereira (2026b)	Apparent models are used for ranking and selectivity, with intercepts and R^2 values reported.
Front-end impurity control	da Silva et al. (2022); Setiawan et al. (2024); Ma et al. (2026)	Fe dissolution is explicitly penalized because it drives neutralization, impurity removal, and solids generation.
Non-sulfuric and combined leaching concepts	Yunita and Mubarok (2021); Acquah et al. (2025)	These studies support the broader view that process intensity should be judged alongside recovery, not in isolation.

The literature comparison shows that the present results are consistent with previous studies on atmospheric sulfuric acid leaching of limonitic and ferruginous lateritic nickel ores. However, the main contribution of this work is not the achievement of the highest nickel extraction, but the development of a transparent decision framework that considers nickel recovery together with Fe dissolution, acid dosage, residence time, and apparent kinetic selectivity.

The selected condition, R800/300, achieved 82.8% Ni extraction while keeping Fe dissolution at 48.4%, a practical compromise between recovery and impurity control. This outcome contrasts with more aggressive leaching approaches that may increase Ni extraction but also intensify Fe dissolution, acid consumption, neutralization demand, and downstream solids generation. Therefore, the present study is best positioned as an atmospheric-leaching screening and decision-support contribution for ferruginous lateritic ores, complementing previous work on kinetics, mineralogical dependence, alternative routes, and impurity-control strategies.

3.8. Reconciled mass-balance check

Table 12 shows a reconciled elemental distribution based on head grades and corrected extraction values, emphasizing the consistent metal-inventory basis and highlighting the importance of dissolved Fe relative to Ni. It is not a substitute for independent raw-stream closure, which should be included in future validation work.

Table 12. Reconciled metal distribution and arithmetic closure check

Condition	Element	Feed (kg/t ore)	Dissolved (kg/t ore)	Residue (kg/t ore)	Closure error (%)
800/300	Ni	10.800	8.942	1.858	0.000

JIRRS
Journal International Review of Research Studies
Received: 02/05/2026 - **Accepted:** 07/07/2026
Vol: 01.09
DOI: 10.66104/dempc459
Pages: 1-30

800/300	Co	0.440	0.218	0.222	0.000
800/300	Fe	335.300	162.285	173.015	0.000
800/300	Mg	26.800	26.800	0.000	0.000
800/300	Mn	6.050	2.396	3.654	0.000
700/420	Ni	10.800	9.169	1.631	0.000
700/420	Co	0.440	0.263	0.177	0.000
700/420	Fe	335.300	164.632	170.668	0.000
700/420	Mg	26.800	26.800	0.000	0.000
700/420	Mn	6.050	2.529	3.521	0.000
900/300	Ni	10.800	8.899	1.901	0.000
900/300	Co	0.440	0.223	0.217	0.000
900/300	Fe	335.300	156.920	178.380	0.000
900/300	Mg	26.800	25.031	1.769	0.000
900/300	Mn	6.050	2.535	3.515	0.000
1000/420	Ni	10.800	9.666	1.134	0.000
1000/420	Co	0.440	0.207	0.233	0.000
1000/420	Fe	335.300	269.581	65.719	0.000
1000/420	Mg	26.800	24.334	2.466	0.000
1000/420	Mn	6.050	2.547	3.503	0.000

Note. Closure error is zero by construction because the table uses head grade and corrected extraction to partition feed inventory into dissolved and residual fractions. Raw independent closure should be reported when all stream masses and assays are finalized.

Limitations and validation requirements

The experimental design is intentionally interpreted as an operational screening study. Only the acid dosage was varied, while the initial ore mass and slurry basis were fixed. Replicate tests, systematic variation of pulp density, particle-size effects, and independent mass-balance closure should be included in future validation work. The R1000 data from 240 to 420 min were retained because they are useful for process interpretation, but they are identified as recalculated values and should be confirmed by repeat testing before being used for detailed engineering design.

Some non-monotonic behavior of Fe is observed, particularly around intermediate residence times. This can reflect analytical uncertainty, heterogeneous residues, secondary precipitation or redistribution of Fe-bearing species, or slurry sampling effects. For this reason, the decision framework uses both concentration-based extraction and process penalties rather than relying only on a single Fe time point.

The main boundary conditions of the framework are as follows: (i) the conclusions are based on one ferruginous lateritic ore fraction; (ii) the experimental matrix varied acid dosage and residence time but did not constitute a full design of experiments; (iii) replicate testing and uncertainty propagation were limited; (iv) Table 9 is an arithmetic partition based on corrected extraction values, not an independent raw-stream closure; (v) raw liquor volumes, wash-water volumes, dry residue masses, residue grades, detection limits, and duplicate assays should be

JIRRS
Journal International Review of Research Studies
Received: 02/05/2026 - **Accepted:** 07/07/2026
Vol: 01.09
DOI: 10.66104/dempc459
Pages: 1-30

provided as supplementary data where disclosure is possible; (vi) economic sensitivity, Fe-removal validation, neutralization demand, and residue-generation tests are still required; and (vii) R800/300 should be confirmed by repeat tests before detailed process design.

The decision framework is transferable as a calculation structure, but the selected operating condition is ore-specific. Other laterite ores, saprolitic blends, finer fractions, or materials with different Mg/Al acid-consuming gangue require recalibration of thresholds, penalty terms, and validation tests.

4. Process Implications

The corrected data sharpens the industrial message. The R1000 condition demonstrates that high nickel extraction alone is not sufficient for process selection. From 240 to 420 min, this condition yields Ni extraction between 83.1% and 89.5%, while Fe dissolution increases from 71.3% to approximately 80.4%. On a one-tonne ore basis, R1000/420 dissolves about 269.6 kg Fe/t ore, compared with about 162.3 kg Fe/t ore at R800/300. This additional Fe load would increase acid demand, neutralization requirements, impurity removal, solid generation, filtration burden, and front-end complexity.

The R700 condition is less aggressive and becomes acceptable at 420 min, but it requires a long residence time to reach the target Ni recovery. The R900 condition reaches the target faster but adds acid without improving the 300 min nickel extraction compared with R800. Therefore, R800 and 300 min is the most balanced practical point within the tested matrix. This conclusion is contingent on the chosen screening limits; if the downstream plant can tolerate higher Fe, then R800/420 or R900/360 may be considered higher-recovery alternatives, but they are not the lowest-penalty options.

5. Conclusions

The corrected extraction values showed that nickel extraction increased with sulfuric acid dosage and residence time. However, this improvement was consistently accompanied by higher iron dissolution. Retaining the corrected R1000 data from 240 to 420 min was important for process interpretation. These data clearly demonstrate the penalty associated with excessive acid dosage.

The R1000 condition achieved relatively high nickel extraction, ranging from 83.1% to 89.5%. Nevertheless, it also resulted in severe Fe dissolution, ranging from 71.3% to 80.4%, indicating poor Ni/Fe selectivity. The R700 condition reached acceptable nickel and iron values only after 420 min. However, this longer residence time increased the process penalty. The R900

JIRRS
Journal International Review of Research Studies
Received: 02/05/2026 - **Accepted:** 07/07/2026
Vol: 01.09
DOI: 10.66104/dempc459
Pages: 1-30

condition achieved high nickel recovery but required a higher acid dosage and exceeded the Fe constraint at longer residence times.

Among the evaluated conditions, R800 at 300 min represented the preferred screening condition and the lowest-penalty acceptable operating point within the tested matrix. This condition achieved 82.8% Ni extraction and 48.4% Fe dissolution. It also presented the lowest penalty index among the acceptable operating points. Apparent kinetic modeling supported this decision framework. R800 provided the best kinetic selectivity among the 700–900 kg H_2SO_4/t ore tests, whereas R1000 showed poor Ni/Fe kinetic selectivity.

Therefore, the proposed framework should be interpreted as an operational decision-support tool for screening and ranking atmospheric leaching conditions, not as final plant design or economic optimization. Before final process design, the selected condition should be validated by replicate tests, independent mass-balance closure, uncertainty propagation, downstream Fe-removal tests, and economic sensitivity analysis.

Declarations

Funding

No external funding is declared for this manuscript draft. If institutional or project funding applies, this statement should be updated before submission.

Conflicts of interest

The authors declare no conflict of interest.

Data availability

The data supporting the findings are derived from laboratory leaching tests, chemical assays, mineralogical characterization, and corrected mass-balance calculations. Processed tables are included in the manuscript; raw laboratory records can be made available upon reasonable request, subject to confidentiality restrictions.

References

1. Abbasi Gharaei, A., Rezai, B., & Hamidian-Shormasti, H. (2024). Environmentally friendly approach: Atmospheric and high-pressure acid leaching studies, low-grade laterite nickel processing. *Journal of Mining and Environment, 15*(4), 1591–1606. https://doi.org/10.22044/jme.2024.14230.2656
2. Acquah, G., Abaka-Wood, G., Skinner, W., Addai-Mensah, J., & Asamoah, R. (2026). Effect of mechanical activation on nickel and cobalt extraction in refractory nickel laterite ore. *Powder Technology, 468*, Article 121655. https://doi.org/10.1016/j.powtec.2025.121655.
3. Acquah, G., Skinner, W., Abaka-Wood, G., Spiridonov, P., Addai-Mensah, J., & Asamoah, R. (2026). Extraction of nickel and cobalt from complex low-grade lateritic ores: Challenges and opportunities. *Minerals, 16*(3), Article 287. https://doi.org/10.3390/min16030287.

JIRRS
Journal International Review of Research Studies

Received: 02/05/2026 - **Accepted:** 07/07/2026
Vol: 01.09
DOI: 10.66104/dempc459
Pages: 1-30

4. Astuti, W., Avista, D., Prihutami, P., Wanta, K. C., Prakosa, A., Anggara, F., & Petrus, H. T. B. M. (2024). Atmospheric leaching behavior and kinetics of nickel and cobalt from Halmahera limonite ore. *International Journal of Technology, 15*(4), 824–833. https://doi.org/10.14716/ijtech.v15i4.5607.
5. Bahfie, F., Manaf, A., Astuti, W., Nurjaman, F., Prasetyo, E., & Herlina, U. (2022). Development of laterite ore processing and its applications. *Indonesian Mining Journal, 25*(2), 89–104. https://doi.org/10.30556/imj.Vol25.No2.2022.1261.
6. Chi, D., Yu, J., Han, Y., Dong, Z., Gao, P., & Li, Y. (2026). Hydrometallurgical technologies of limonitic nickel laterite ore for carbon-neutral metallurgy: A review. *JOM*. Advance online publication. https://doi.org/10.1007/s11837-026-08139-2.
7. Dahani, W., Jaksa, I. G. N. B. S., Marwanza, I., Kurniawati, R., & Subandrio, S. (2020). The effect of pre-roasting on nickel extraction from limonite ore by acid leaching method. *AIP Conference Proceedings, 2267*, Article 020042. https://doi.org/10.1063/5.0015935.
8. da Silva, M. de F., Oliveira, M. R. de S., dos Santos, I. D., Radino-Rouse, P. (2022). Iron precipitation strategies from nickel laterite ore sulfuric acid leach liquor. *Mineral Processing and Extractive Metallurgy Review, 43*(1), 1–12. https://doi.org/10.1080/08827508.2020.1809392.
9. Eljoudiani, A., Sampaio, C. H., Oliva, J., Veras, M. M., Alfonso, P., Anticoi, H., Tampouris, S., Cortina, J. L., & Escalante, P. R. (2024). Technological characterization of cobalt and nickel ores from Greece for metal recovery. *Separations, 11*(12), Article 345. https://doi.org/10.3390/separations11120345.
10. Hariyanto, R.K.S., Tomas Da Rocha, L., Kim, S.J. *et al.* Extraction Behavior of Nickel and Cobalt From Serpentine-Rich Ore Through Sulfation–Roasting–Leaching Process. *Metall Mater Trans B* **54**, 2915–2928 (2023). https://doi.org/10.1007/s11663-023-02934-x
11. Hosseini Nasab, M., Noaparast, M., & Abdollahi, H. (2020). Dissolution optimization and kinetics of nickel and cobalt from iron-rich laterite ore, using sulfuric acid at atmospheric pressure. *International Journal of Chemical Kinetics, 52*, 283–298. https://doi.org/10.1002/kin.21349.
12. Jeong, H.-E., Kang, H., Choi, S., & Kim, H. (2025). Comparative study of limonitic and saprolitic laterite ores on the leaching characteristics under atmospheric pressure. *Minerals Engineering, 226*, Article 109250. https://doi.org/10.1016/j.mineng.2025.109250.
13. Kang, H., Kim, J., Lee, J., Lee, D., Ko, D., & Kim, H. (2026). Early-stage temperature-dependent leaching kinetics and mechanisms of saprolitic and limonitic nickel laterite ores under atmospheric conditions. *Minerals Engineering, 239*, Article 110115. https://doi.org/10.1016/j.mineng.2026.110115.
14. Li, G., Chen, Y., Mang, C., Teng, X., **[dois autores adicionais a confirmar]**. (2023). Near-zero-waste approach for the treatment of saprolitic nickel laterite via a combined hydrometallurgical process. *ACS Sustainable Chemistry & Engineering, 11*(18). https://doi.org/10.1021/acssuschemeng.2c05403
15. Li, Z. X., Liu, Y. L., Chang, J., Ju, X. T., Huang, J., Li, J. F., ... & Yang, Z. B. (2026). Sulfation roasting of the nickel laterite ore: ammonia leaching kinetics study in selective Ni extraction. *Canadian Metallurgical Quarterly*, *65*(2), 2021-2031..
16. Ma, H., Zhang, X., Wang, Y., Bai, P., . (2026). Atmospheric sulfuric acid leaching of metals from nickel laterite and selective phosphate precipitation of $FePO_4$. *Hydrometallurgy, 244*, Article 106812. https://doi.org/10.1016/j.hydromet.2026.106812.
17. Osali, M., Ahani, F., Aboutalebi, M. R., Adeli, M., Moghaddam, J., Karimi, S., Wijenayake, J. J., & Alagha, L. (2026). Selective extraction of nickel and cobalt from limonitic laterite via optimized sulfation roasting–water leaching and solvent extraction. *Minerals, 16*(5), Article 431. https://doi.org/10.3390/min16050431.

JIRRS
Journal International Review of Research Studies

Received: 02/05/2026 - **Accepted:** 07/07/2026
Vol: 01.09
DOI: 10.66104/dempc459
Pages: 1-30

18. Pandey, N., Tripathy, S. K., Patra, S. K., & Jha, G. (2023). Recent progress in hydrometallurgical processing of nickel lateritic ore. *Transactions of the Indian Institute of Metals, 76*(1), 11–30. https://doi.org/10.1007/s12666-022-02706-2.
19. Pereira, A. C. (2026a). From mineralogy to process design: The role of particle size distribution on nickel extraction kinetics and hydrometallurgical route selection in a limonitic laterite. IKR Journal of Engineering and Technology, 2(4). https://doi.org/10.5281/zenodo.21209619
20. Pereira, A. C. (2026b). Bottle roll tests for kinetic evaluation of nickel ores: Capabilities, limitations, and misinterpretations – A critical review. REMUNOM, 13(7). https://doi.org/10.66104/z4cay337.
21. Prameswara, G., Tyassena, F. Y. P., Pasaribu, M., Trisnawati, I., & Petrus, H. T. B. M. (2023). Nickel recovery optimization and kinetic study of Morowali laterite ore. Transactions of the Indian Institute of Metals, 76, 1341–1348. https://doi.org/10.1007/s12666-022-02858-1.
22. Prameswara, G., Amin, I., Ulfah, A. N., Trisnawati, I., Petrus, H. T. B. M., & Puspita, F. (2024). Atmospheric leaching behavior and kinetics study of roasted laterite ore. Mining, Metallurgy & Exploration, 41, 1025–1033. https://doi.org/10.1007/s42461-024-00947-x.
23. Prasetya, A., Putera, A. D. P., Sujoto, V. S. H., Zaidan, M. H., Abdurrahman, M. T., Andriani, A., Astuti, W., Sutijan, & Petrus, H. T. B. M. (2025). Enhanced recovery of nickel and cobalt from limonitic laterite ore: Optimization and kinetics of atmospheric sulfuric acid leaching. Journal of Sustainable Metallurgy, 11(4), 4127–4140. DOI: 10.1007/s40831-025-01231-y.
24. Ribeiro, G. da S., de Deus Nascimento, N., da Silveira Ribeiro, R., de Paole Moreira Miranda, M., Martins, P. R., Costa Caetano, G., Alves de Andrade, L., & Ostroski, I. C. (2025). Optimization of the atmospheric acid leaching process for the recovery of nickel and cobalt from iron-rich lateritic ore. Mining, Metallurgy & Exploration, 42(2), 1127–1140. https://doi.org/10.1007/s42461-025-01233-0
25. Ribeiro, P. P. M., de Souza, L. C. M., Neumann, R., dos Santos, I. D., & Dutra, A. J. B. (2020). Nickel and cobalt losses from laterite ore after the sulfation-roasting-leaching processing. Journal of Materials Research and Technology, 9(6), 12404–12415. https://doi.org/10.1016/j.jmrt.2020.08.082.
26. Ribeiro, P. P. M., dos Santos, I. D., Neumann, R., Fernandes, A., & Dutra, A. J. B. (2021). Roasting and leaching behavior of nickel laterite ore. Metallurgical and Materials Transactions B, 52(3), 1739–1754. https://doi.org/10.1007/s11663-021-02141-6.
27. Safitri, N., Mubarok, M. Z., Meidji, I. U., Hardi, J., & Jayadi, H. (2021). Leaching of limonitic nickel from Sorowako with sulfuric acid at atmospheric pressure. Journal of Physics: Conference Series, 1763(1), Article 012044. DOI: 10.1088/1742-6596/1763/1/012044.
28. Santos, A. L. A., Becheleni, E. M. A., Viana, P. R. M., Papini, R. M., Silvas, F. P. C., & Rocha, S. D. F. (2021). Kinetics of atmospheric leaching from a Brazilian nickel laterite ore allied to redox potential control. Mining, Metallurgy & Exploration, 38, 187–201. https://doi.org/10.1007/s42461-020-00310-w.
29. Setiawan, I., Nabilah, A., Oediyani, S., Subagja, R., Irawan, J., Sampoerno, A. B., Yunita, F. E., Suharyanto, A., & Syahid, A. N. (2023). Kinetic of dissolution of nickel limonite calcine by sulfuric acid solution. Jurnal Metalurgi, 38(3), 109–116. https://doi.org/10.55981/metalurgi.2023.740.
30. Setiawan, I., Oediyani, S., Setiawati, N., Irawan, J., Subagja, R., Rhamdani, A. R., & Lalasari, L. H. (2024). Iron precipitation from nickel laterite ores using sulfuric acid atmospheric leaching with addition of hydrogen peroxide. AIP Conference Proceedings, 3003(1), Article 020094. https://doi.org/10.1063/5.0186246.

JIRRS
Journal International Review of Research Studies

Received: 02/05/2026 - **Accepted:** 07/07/2026
Vol: 01.09
DOI: 10.66104/dempc459
Pages: 1-30

31. Stanković, S., Stopić, S., Sokić, M., Marković, B., & Friedrich, B. (2020). Review of the past, present, and future of the hydrometallurgical production of nickel and cobalt from lateritic ores. Metallurgical and Materials Engineering, 26(2), 199–208. https://doi.org/10.30544/513.
32. Tyassena, F. Y. P., AL, M. D. Z., Abrilla, A. M. A., Sarwana, W., Setyorini, D., Syafaatullah, A. Q., Ganing, M., Arninda, A., Rahim, H., & Prameswara, G. (2026). Optimizing microwave-assisted leaching of nickel from laterite ores: RSM-based modeling and kinetics. Chemical Papers. Advance online publication. https://doi.org/10.1007/s11696-026-04911-5.
33. Wang, Y., Wu, Y., Fan, Y., Wang, Y., & Li, L. (2024). Leaching kinetics of limonite-type laterite nickel ore from ammonium hydrogen sulfate solution at atmospheric pressure. JOM, 76(11), 6363–6375. https://doi.org/10.1007/s11837-024-06470-0.
34. Wanta, K. C., Astuti, W., Perdana, I., & Petrus, H. T. B. M. (2020). Kinetic study in atmospheric-pressure organic acid leaching: Shrinking core model versus lump model. Minerals, 10(7), Article 613. https://doi.org/10.3390/min10070613
35. Yunita, F. E., & Mubarok, M. Z. (2021). Nickel leaching from laterite ores by the combination of organic and sulfuric acid. AIP Conference Proceedings, 2382(1), 050003. DOI: 10.1063/5.0060750.
36. Zablotskaya, Y. V., Sadykhov, G. B., Olyunina, T. V., Khasanov, M. Sh., & Smirnova, V. B. (2020). Some features of the sulfuric acid leaching of the reduced ferriferous oxidized nickel ore. Russian Metallurgy (Metally), 2020, 1472–1476. https://doi.org/10.1134/S0036029520130406
37. Zablotskaya, Y. V., Sadykhov, G. B., Anisonyan, K. G., Smirnova, V. B., & Tuzhilin, A. S. (2022). On the problem of enhancing selectivity of nickel and cobalt recovery during the sulfuric acid leaching of reduced oxidized nickel ore. Russian Metallurgy (Metally), 2022(9), 985–989. DOI: 10.1134/S0036029522090142
38. Zhao, Z., Li, H., & Wang, C. (2025). An integrated sulfation-roasting-leaching process for coextraction of nickel and cobalt from laterite ores with enhanced SO_3 recovery. ACS Sustainable Resource Management, 2(1), 201–211. https://doi.org/10.1021/acssusresmgt.4c00437.